International Journal of Mechanical and Production Engineering Research and Development (IJMPERD)
ISSN (P): 2249-6890; ISSN (E): 2249-8001
Vol. 8, Issue 4, Aug 2018, 855-862

EFFECT OF GMAW PROCESS PARAMETERS ON IS 2062 STEEL CLAD GEOMETRY

G. BRITTO JOSEPH & T. N. VALARMATHI

Department of Mechanical Engineering, Sathyabama Institute of Science and Technology, Chennai, Tamil Nadu, India

ABSTRACT

In the present-day fabrication industries, the automatic welding plays an important role. The quality of welding depends on the welding process welding, so the influence of parameters and their interactions decide the sound of the welding. The mathematical model is developed to determine the influence of parameters and its interaction between them. GMAW is preferred by the manufacturing and fabrication industries due to the smooth finish, high productivity, and deep penetration. A factorial design is engineered for IS 2062 steel plates using the RSM-CCD technique by considering four factors and five levels to forecast the dimensions of the clad bead geometry and the interaction of process parameters. The interaction of the process parameters is presented in graphical form. By using this, clad bead geometry and quality of the cladding process parameters are analyzed.

***KEYWORDS**: Weld Bead Geometry, GMAW & Mathematical Modelling*

Received: Jun 13, 2018; **Accepted:** Jul 03, 2018; **Published:** Jul 31, 2018; **Paper Id.:** IJMPERDAUG201888

Original Article

1. INTRODUCTION

Automated welding is widely used now for manufacturing and fabrication industries to achieve precision and higher production. For the quality clad, it is very important to control the process parameters. Controlling the process parameters is achieved by knowing their influence of the process parameters and their interactions between other parameters to get the quality clad bead geometry in automated welding [1]. GMAW has been widely used in fabrication industries in view of their advantages of high productivity, ease of work, low cost, high deposition, low cost, flux absences, cleanliness, welded both ferrous and nonferrous metals [2]. The mechanical strength and quality of the clad does not only depend on the chemical composition of the metals but also depends on the process parameters of the clad [3 -4]. Weld geometry is the formation of weld bead shape. Weld bead shape depends on the factors such as heat energy supplied from the arc to metal of base per unit length, joint preparation, welding speed, etc. So characteristics of the shape of the weld bead are very much important. To achieve the desired weld bead shape, a study of the effect of process parameters and its interaction controlling the weld bead shape is to be recognized. Mathematical models developed by the design of experiment helped to predict the weld bead geometries (weld bead width, reinforcement and penetration) and also the design of the experiment is used for optimizing the welding process parameters to achieve the desired the shape with quality cladding.

Mathematical models developed by the full factorial statistically designed experiments techniques [5]. Required details about the influence welding process parameters and interaction of the welding process parameters are predicted by these mathematical models. The mathematical models were developed by measuring weld bead

width, reinforcement, and penetration of the various cladded metals. The final model of the work was developed by the regression analysis and the developed model's significance is verified by the ANOVA technique [6]. The effect or influence of the cladding process parameters and the interaction of process parameters were analyzed from the clad bead measurement and presented in graphical form.

1.1. Experimental Design and Execution

The following steps were carried out to do the experimental work shown in figure 1.

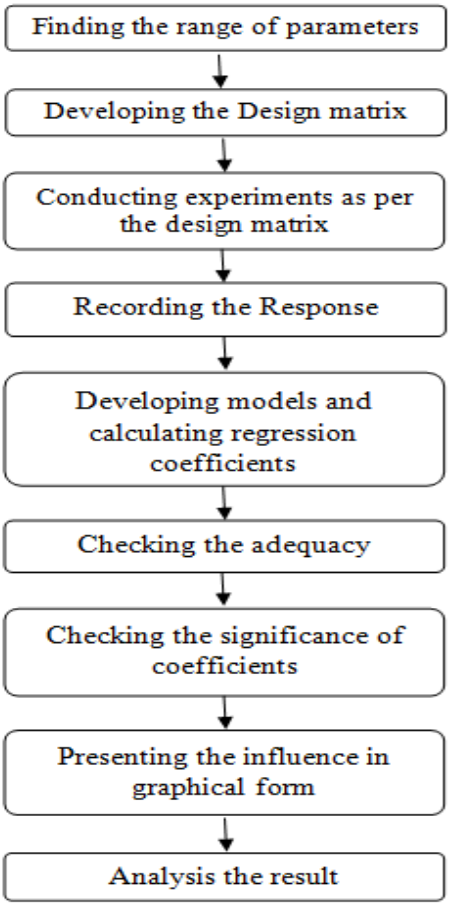

Figure 1: Flow Diagram of the Experimental Work

2. EXPERIMENTAL WORK

Thyro µP 400 used to carry out the experiments using DC and considering electrode is positive. A test piece of size 200×100×15 mm cut by water jet machining and all test pieces were grounded and clean surface to free from oxide scale and dirt before cladding. The IS 2062 metal used as a base metal and filler is ER 308l. The chemical composition of the base metal IS 2062 and filler ER 308l are given in table 1.

Table 1: Chemical Composition of Base Metal and Filler Wire

Material	C	Si	Mn	P	S	Al	Cr	Ni
Is 2062	0.14	0.15	0.86	0.014	0.015	0.03	-	-
ER 308L	0.02	0.56	1.75	0.02	0.007`	-	19.51	10.01

3. PLAN FOR DESIGN

3.1. Finding the Input Process Parameters First, the input of the welding process parameters is identified. The important welding process parameters are 1. Speed of the welding, 2. Current, and 3. Nozzle to Plate distance

3.2. The Ranges (Upper Limit and Lower Limit) of those Welding Process Parameters were Identified

The ranges of the welding process parameters were identified first. One weld bead is overlaid on the base metal by changing one of the welding process parameters while keeping the remaining welding process parameters were constant. By observing the visual defects and smooth appearance of the weld bead, the ranges of each welding process parameters were found. The in-between values were calculated by the following equation

$$Yi = \frac{2[2Y-(Ymax+Ymin)]}{Ymax-Ymin} \quad (1)$$

Where Yi is the needed coded value of a parameter Y. Y is any value of the parameter from Ymin to Ymax, Ymin is the lower limit of the parameter, and Ymax is the upper limit of the parameter. The chosen levels of the selected process parameters along with their units and notations are represented in table 2.

Table 2: Chosen Cladding Parameters and Their Levels

Parameter	Unit	Factors Levels		
		-1	0	1
Current	Amps	190	210	230
Welding speed	m/min	5.9	6.9	7.9
Nozzle to plate distance	mm	5.9	6.9	7.9

3.3. Development of Design Matrix and Recording the Responses like Width, Reinforcement, and Penetration

The design matrix developed by the RSM-CCD technique is given in table 3. Based on the table, all the experiments were carried out. After every run, the setting of the welding parameters changed and arranged it for the new set welding parameters overlay given in table 3. All the specimen after the single overlay were grounded, polished and etched with 2% nital. Optical profile projector used to measure the weld bead shape after the single overlay. The width of the weld bead, reinforcement, and penetration of the welded bead were measured by using the optical profile projector.

Table 3: Design Matrix

Run	A:Current A	B:Welding Speed m/min	C:Nozzle to Plate Distance mm	Penetration mm	Reinforcement mm	Width Mm
1	230	7.9	22	1.08	4.63	12.53
2	190	5.9	24	0.88	4.74	9.85
3	210	7.9	20	0.93	4.34	10.58
4	210	6.9	20	1.07	4.46	10.62
5	230	6.9	24	1.15	4.83	12.13
6	190	5.9	20	0.98	4.59	9.4
7	210	5.9	22	1.06	5.12	11.8
8	190	7.9	22	0.94	4.21	8.88
9	210	6.9	22	1.12	4.66	10.82
10	210	6.9	22	1.13	4.59	10.85
11	210	6.9	24	0.97	4.62	10.92
12	190	7.9	24	0.82	4.12	9.4
13	210	6.9	22	1.13	4.58	10.81

Table 3: Contd.,						
14	230	7.9	24	1	4.64	12.54
15	230	7.9	20	1.08	4.37	12.4
16	230	5.9	20	1.19	4.91	13.76
17	190	7.9	20	0.91	4.09	8.15

3.4. Mathematical Models were Developed based on their Responses

The response function for three process parameters of a weld bead can be represented in following form (8)

$$Z = f(Y1, Y2, Y3) \quad (2)$$

Where Z is the response (e.g., weld bead width), Y_1 – Welding Current, Y_2 – Voltage, Y_3 – Welding speed. The second order polynomial equation used for the three factors can be represented in the following equation

$$Y = \lambda 0 + \lambda 1A + \lambda 2B + \lambda 3C + \lambda 11A2 + \lambda 22B2 + \lambda 33C2 + \lambda 12AB + \lambda 13AC + \lambda 23BC \quad (3)$$

Where λ_0 is the free coefficient of the polynomial equation. λ_1, λ_2, and λ_3 are linear terms. λ_{11}, λ_{22} and λ_{33} are quadratic terms. λ_{12}, λ_{13}, & λ_{23} are interaction terms.

3.5. Verifying the Adequacy of the Mathematical Model

Usually, regression analysis used to find the values of the regression coefficients. The standard deviation value of from the ANOVA table 4 must be above 95%. The scatter diagram shows the deviation of actual values from theoretical values.

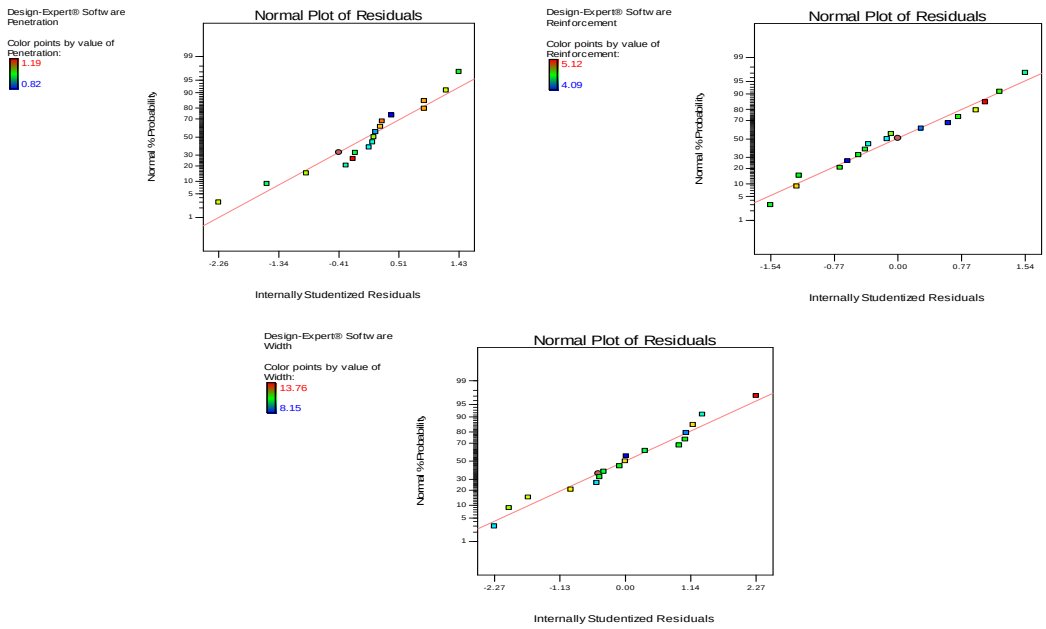

Figure 2: Scatter Diagram

Table 4(a): Anova Table

ANOVA for Response Surface Quadratic Model						
Analysis of Variance Table [Partial Sum of Squares - Type III]						
Source	**Sum of Squares**	**df**	**Mean Square**	**F Value**	**P value Prob > F**	
Model	0.179358	9	0.019929	67.915	< 0.0001	significant
A-Current	0.066695	1	0.066695	227.2904	< 0.0001	
B-Welding speed	0.017166	1	0.017166	58.49924	0.0001	
C-Nozzle to Plate distance	0.017656	1	0.017656	60.17156	0.0001	
AB	0.001097	1	0.001097	3.73773	0.0945	
AC	5.48E-05	1	5.48E-05	0.186871	0.6785	
BC	3.04E-05	1	3.04E-05	0.103711	0.7568	
A^2	0.00656	1	0.00656	22.35536	0.0021	
B^2	0.018582	1	0.018582	63.32604	< 0.0001	
C^2	0.021	1	0.021	71.56605	< 0.0001	
Residual	0.002054	7	0.000293			
Lack of Fit	0.001987	5	0.000397	11.92427	0.0792	not significant
Pure Error	6.67E-05	2	3.33E-05			
Cor Total	0.181412	16				

Table 4(b)

Std. Dev.	0.01713	R-Squared	0.988677
Mean	1.025882	Adj R-Squared	0.97412
C.V. %	1.669777	Pred R-Squared	0.951063

4. RESULTS AND DISCUSSIONS

To predict the clad bead geometry and its shape relationships the mathematical models developed

4.1. Direct Effect of Current on Clad Bead Geometry

Figure 3(a) shows the direct effect of welding current. Process parameter current in gas metal arc welding plays an important role during welding. This current effect the deposition of weld bead width, penetration and reinforcement. When current is more than the optimum value, increases the width of weld bead, penetration, and reinforcement. As a result, wastage of the filler metal is also high. Very low current during welding produces poor penetration and increases the pileup by means of overlay on the base metal. As a result, the bead is rough and increases the reinforcement. Hence high current or low current in welding affect the mechanical properties of weld metal [9].

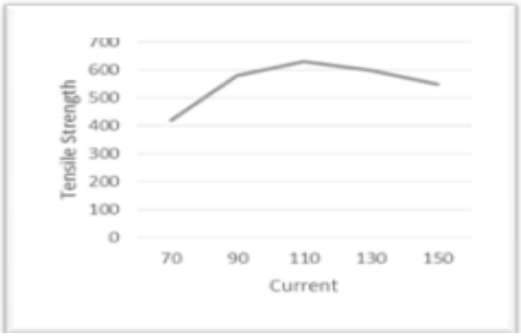

Figure 3(a): Direct Effect of Current

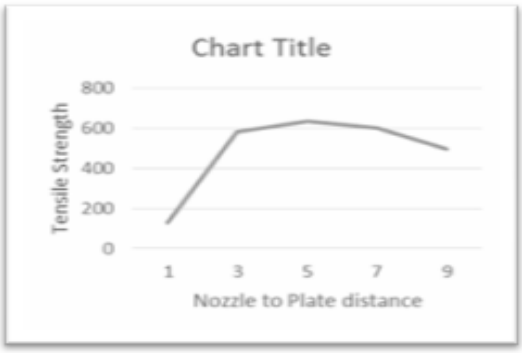

Figure 3(b): Direct Effect of Nozzle to Plate Distance

4.2 Direct Effect of Nozzle to Plate Distance on Clad Bead Geometry

Figure 3(b) shows the direct effect of the nozzle to plate distance. It is obvious that the depth of penetration inversely proportional to the distance between the nozzle and the plate. But if the distance between the nozzle and plate increases the clad bead width and reinforcement also increases. This is due to the circuit resistance increases when the nozzle to plate distance increases, which diminishes the electrical current. Heat input to the weld metal also reduces when the electrical current reduces. Therefore depth of penetration decreases when the distance between the nozzle and plate increases [10].

4.3 Direct Effect of Welding Speed on Clad Bead Geometry

Figure 3(c) shows the direct effect of welding speed. Reinforcement and weld bead width decreases with increasing welding speed. This is due to reduce in heat input per unit length of the clad bead. But the depth of penetration reduces with increasing the welding speed. When welding speed is low, the arc of the system is almost vertical and stops the deep penetration [11].

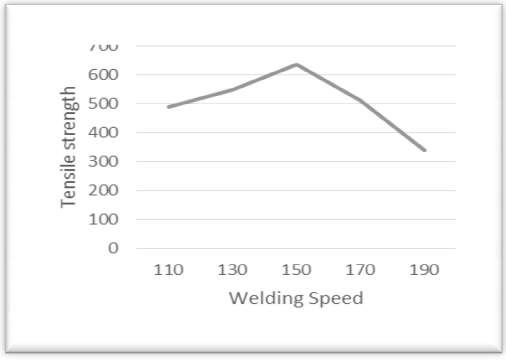

Figure 3 (c): Direct Effect of Welding Speed Effect

4.4 Interaction between Welding Speed and Current

From the figure 4 it clear that increases of penetration occurs when increases in current and decreases the welding speed. This is because of heat input reduction when the welding speed increases. This is due to the positive effect of welding speed and weld current. From the figure, it is clear that, reinforcement decreases with decreasing the current. This is due to low heat input to the welded metal. This is due to the positive effect of weld current [13].

4.5 Interaction between Nozzle to Plate Distance and Welding Speed

Figure 4 clearly shows that penetration decreases with increases in welding speed and increasing nozzle to plate distance. This is due to lesser heat input when welding speed increases and nozzle to plate distance increases to the welding process. This is to the positive effect of the nozzle to plate distance [14].

4.8 Interaction between Welding Speed and Nozzle to Plate Distance

From the figure 4, it is clear that the depth of penetration, reinforcement and weld bead width decreases with increasing in welding speed and nozzle to plate distance. This is due to, low heat input per unit length of the base metal and the negative effect of welding speed and nozzle to plate distance [16].

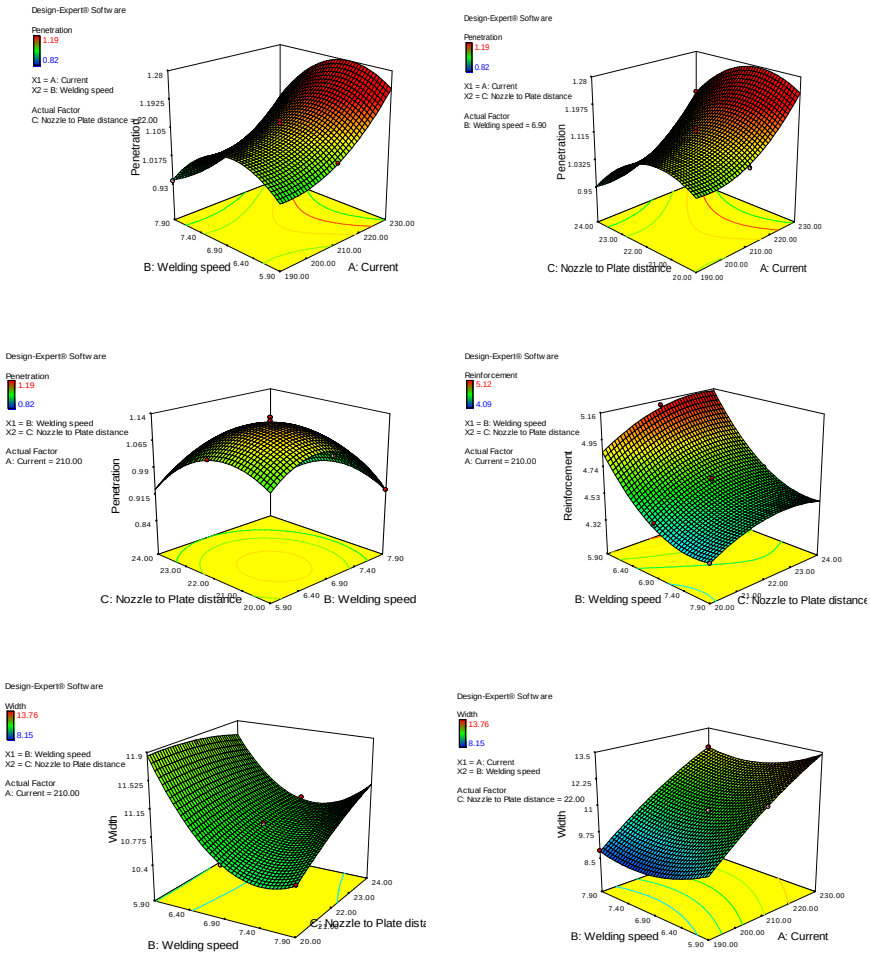

Figure 4: Interaction between the Parameters

CONCLUSIONS

- The main purpose of this cladding work is to get the maximum penetration. This can be concluded that the response surface method is a powerful tool to get the optimum clad geometry.
- The actual results of this experiment are close the prediction results which developed by the mathematical models.
- The clad bead width, penetration and reinforcement increases with increases in welding current.
- A height of the reinforcement and weld bead width decreases with increasing welding speed.

- A height of the reinforcement and weld bead width increases by increasing the distance between the plate and nozzle tip.
- Clad bead width increases with decreasing the welding speed.
- Penetration increases with decreasing the welding speed and increasing the welding current

REFERENCES

1. *M.M. Chakrabarty, Chemistry and Technology of Oils & Fats, 81-7764-495-5(2003) 3-13*
2. *M.C. Teale, P.C. Colder, T.R. Dhiman, G. Bienkiewiez, Z. Domiszewski, J. Dunstan, T. Furuta, Omega 3 Fatty Acid Research, ISBN:1-59454-620-7 (2006) 1-25.*
3. *P. Manzano, J.C. Diego, M.J. Nozal, J.L. Bernal, Food .Comp. Analy. 28 (2012) 31-32.*
4. *M. Milovanoviel, P.J.A. Ksenija, Science 50 (2005) 41-47.*
5. *M.H. Coleman, Advan. Lipid. Resea. 1 (1963)1.*
6. *F.D. Gunstone, F.B. Padley, M.I. Qureshi, Chem. Ind. 483 (1964) 345.*
7. *G. Britto Joseph, G. Mageshwaran, Jeya Jeevahan, R. B. Durai Raj, and A. Poovannan, International Journal Of Ambient Energy, DOI: 10.1080/01430750.2017.1399460, 2017*
8. *A.R.S. Kartha, Amer. Oil. Chem. Society. 08 (1953) 88.*
9. *R.J. Vanderwal, Amer. Oil. Chem. Society.70 (1960) 11.*
10. *El-Bitar, T. A. H. E. R., M. A. H. A. El-meligy, and E. M. A. N. El-Shenawy. "Physical simulation for hot rolling policy of electrical Si-steels." International Journal of Mechanical and Production Engineering Research and Development 7 (2017): 221-230.*
11. *A. Chehma, Catalogue des plantes spontanées du Sahara septentrional Algérienne. 9947 (2006) 75.*
12. *F.O. Urukpa, R.E. Aluko, Food. Chem. 87 (2004) 349-350.*
13. *I.A. Nehdi, H. Sbihi, C.P. Tan, S.I. Al-resayes, Food. Chem. 136 (2013) 349.*
14. *M.A. Soliman, A.A. Elsawy, H.M. Fadel, F. Osman, A.M. Gad, Agro. Biol. Chem. 49 (1985) 269.*
15. *J. Berhaut, Flor .Illu .Sene. 324 (1975) 634.*
16. *G.I.O. Badifu, A.O. Ogunsua, Plan. Food. Hum. Nutr. 41 (1991) 35.*